Overcoming Gemcitabine Resistance in Pancreatic Cancer Using the BCL-X_L–Specific Degrader DT2216

Dinesh Thummuri[1], Sajid Khan[1], Patrick W. Underwood[2], Peiyi Zhang[3], Janet Wiegand[1], Xuan Zhang[3], Vivekananda Budamagunta[1], Amin Sobh[4], Abderrahmane Tagmount[4], Alexander Loguinov[4], Andrea N. Riner[2], Ashwin S. Akki[5], Elizabeth Williamson[6], Robert Hromas[6], Christopher D. Vulpe[4], Guangrong Zheng[3], Jose G. Trevino[2,7], and Daohong Zhou[1]

ABSTRACT

Pancreatic cancer is the third most common cause of cancer-related deaths in the United States. Although gemcitabine is the standard of care for most patients with pancreatic cancer, its efficacy is limited by the development of resistance. This resistance may be attributable to the evasion of apoptosis caused by the overexpression of BCL-2 family antiapoptotic proteins. In this study, we investigated the role of BCL-X_L in gemcitabine resistance to identify a combination therapy to more effectively treat pancreatic cancer. We used CRISPR-Cas9 screening to identify the key genes involved in gemcitabine resistance in pancreatic cancer. Pancreatic cancer cell dependencies on different BCL-2 family proteins and the efficacy of the combination of gemcitabine and DT2216 (a BCL-X_L proteolysis targeting chimera or PROTAC) were determined by MTS, Annexin-V/PI, colony formation, and 3D tumor spheroid assays. The therapeutic efficacy of the combination was investigated in several patient-derived xenograft (PDX) mouse models of pancreatic cancer. We identified BCL-X_L as a key mediator of gemcitabine resistance. The combination of gemcitabine and DT2216 synergistically induced cell death in multiple pancreatic cancer cell lines *in vitro*. *In vivo*, the combination significantly inhibited tumor growth and prolonged the survival of tumor-bearing mice compared with the individual agents in pancreatic cancer PDX models. Their synergistic antitumor activity is attributable to DT2216-induced degradation of BCL-X_L and concomitant suppression of MCL-1 by gemcitabine. Our results suggest that DT2216-mediated BCL-X_L degradation augments the antitumor activity of gemcitabine and their combination could be more effective for pancreatic cancer treatment.

Introduction

Pancreatic cancer is one of the most aggressive human cancers with a 5-year survival rate of approximately 9% and a median survival of <11 months in the United States (1–3). It is the third most common cause of cancer-related deaths. Gemcitabine, a deoxycytidine analogue that inhibits DNA replication, is currently the first-line standard of care chemotherapy for pancreatic cancer. Unfortunately, the therapeutic efficacy of gemcitabine is limited by the innate and acquired resistance leading to treatment failure and recurrent disease in most patients (4–7). Although FOLFIRINOX (a combination of 5-fluorouracil, leucovorin, irinotecan, and oxaliplatin) treatment has increased the survival of patients with high-grade pancreatic cancer compared with gemcitabine, it is associated with increased toxicities and a decreased quality of life (8, 9). Therefore, the identification of the molecular basis of gemcitabine resistance and developing rational combination therapies that can more effectively treat pancreatic cancer are of a critically unmet medical need.

BCL-2 family antiapoptotic proteins (BCL-2, BCL-X_L, and MCL-1) are involved in cancer progression and resistance to chemotherapy and radiation. Among these antiapoptotic proteins, BCL-X_L plays a crucial role in pancreatic cancer (5, 10, 11). Previous reports have shown that in pancreas-specific $KRAS^{G12D}$ mice, BCL-X_L expression was gradually increased during the progression of pancreatic intraepithelial neoplasia (PanIN) to pancreatic ductal adenocarcinoma (PDAC; ref. 12). Another study showed that tumor tissues from approximately 90% of patients with pancreatic cancer expressed increased levels of BCL-X_L (13). These high levels of BCL-X_L in pancreatic cancer have been shown to be associated with gemcitabine resistance; therefore, BCL-X_L inhibition sensitizes pancreatic cancer cells to gemcitabine treatment (14–17). Unfortunately, the direct targeting of BCL-X_L with a conventional small-molecule inhibitor is not a clinically viable approach due to the on-target and dose-limiting thrombocytopenia caused by BCL-X_L inhibition in platelets (18, 19). Recently, using emerging Proteolysis Targeting Chimera (PROTAC) technology, we successfully converted ABT263 (a BCL-X_L/2 inhibitor) into DT2216, a platelet-sparing BCL-X_L-selective PROTAC that targets BCL-X_L to the Von Hippel-Lindau (VHL) E3 ligase for ubiquitination and proteasomal degradation (20). DT2216 has shown promising antitumor activities in BCL-X_L–dependent hematologic malignancies when used as single-agent therapy and in multiple solid tumors when combined with conventional chemotherapy (20–22). Therefore, it has recently been authorized as an investigational new drug for dose-finding clinical trials by the FDA

[1]Department of Pharmacodynamics, College of Pharmacy, University of Florida, Gainesville, Florida. [2]Department of Surgery, College of Medicine, University of Florida, Gainesville, Florida. [3]Department of Medicinal Chemistry, College of Pharmacy, University of Florida, Gainesville, Florida. [4]Department of Physiological Sciences, College of Veterinary Medicine, University of Florida, Gainesville, Florida. [5]Department of Pathology, College of Medicine, University of Florida, Gainesville, Florida. [6]Department of Medicine, University of Texas Health Science Center at San Antonio, San Antonio, Texas. [7]Division of Surgical Oncology, School of Medicine, Virginia Commonwealth University, Richmond, Virginia.

Note: Supplementary data for this article are available at Molecular Cancer Therapeutics Online (http://mct.aacrjournals.org/).

D. Thummuri, S. Khan, and P.W. Underwood contributed equally to this article.

Corresponding Author: Daohong Zhou, Department of Pharmacodynamics, College of Pharmacy, University of Florida, Gainesville, FL 32611. Phone: 352-294-8952; Fax: 352-273-7705; E-mail: zhoudaohong@cop.ufl.edu

Mol Cancer Ther 2022;21:184–92

doi: 10.1158/1535-7163.MCT-21-0474

(NCT04886622). The lack of single-agent efficacy of DT2216 in solid tumors is mainly due to redundant expression of BCL-2, BCL-X_L, and MCL-1 in these tumors, which makes them codependent on two or more of these proteins (23–26). This is because the interaction of proapoptotic proteins (e.g., BIM) with multiple partners may lead to these proapoptotic proteins switching interaction between different antiapoptotic proteins upon single inhibitor treatment. For instance, the displacement of BIM from BCL-X_L and BCL-2 by ABT263 treatment led to its increased association with MCL-1 (27, 28). These findings underscore the importance of cotargeting multiple antiapoptotic BCL-2 proteins for effective antitumor therapy.

To identify druggable genes important to and commonly involved in the development of gemcitabine, 5-fluorouracil (5FU), and niraparib resistance in pancreatic cell lines, we conducted CRISPR screening using a custom library targeting drug targets, termed the Therapeutic Genome (RxG) Library. We found the *BCL2L1* gene that encodes BCL-X_L is important in providing resistance to these three agents. We selected gemcitabine to study in combination with DT2216 against various established and primary pancreatic cancer cells *in vitro* and *in vivo* in a xenograft mouse model, as well as in patient-derived xenograft (PDX) mouse models. We observed that the DT2216–gemcitabine combination synergistically kills various pancreatic cancer cells *in vitro*. More importantly, the combination was found to be more effective than the individual agents at inhibiting tumor growth and increasing the survival of the mice without causing any significant normal tissue toxicities. Our mechanistic investigation revealed that the downregulation of MCL-1 by gemcitabine coupled with BCL-X_L degradation by DT2216 are implicated in their synergistic activity. Collectively, our results suggest that the combination of gemcitabine and DT2216 can synergistically suppress pancreatic tumor growth, and therefore, may reduce resistance to gemcitabine.

Materials and Methods

Cell culture

AsPC-1 (catalog No. CRL-1682), BxPC3 (catalog No. CRL-1687), Mia PaCa2 (catalog No. CRL-1420), and PANC-1 (catalog No. CRL-1469) human pancreatic cancer cell lines were purchased from the ATCC. G-46 and G-68 patient-derived primary pancreatic cancer cell lines were established, characterized, and authenticated using methods described previously (29, 30). PANC-1 and Mia PaCa2 cells were cultured in DMEM (catalog No. 12430054, Thermo Fisher Scientific). AsPC-1 and BxPC3 cells were cultured in RPMI medium (catalog No. 22400–089, Thermo Fisher Scientific). G-46 and G-68 cells were cultured in advanced DMEM medium (catalog No. 12430054, Thermo Fisher Scientific). All the cell lines were cryopreserved from early passages and were cultured for no more than 12 passages following thawing. Cell lines were authenticated prior to use by short tandem repeat (STR) profiling. Cultures were confirmed for *Mycoplasma* negativity using the MycoAlert Mycoplasma Detection Kit (catalog No. LT07–318, Lonza). All culture mediums were supplemented with 10% heat-inactivated FBS (catalog No. S11150H, Atlanta Biologicals), 100 U/mL penicillin and 100 μg/mL streptomycin (Pen-Strep, catalog No. 15140122, Thermo Fisher Scientific). All the cell lines were maintained in a humidified incubator at 37° C and 5% CO_2.

Chemical compounds

DT2216 was synthesized in Dr. Guangrong Zheng's laboratory (University of Florida, Gainesville, FL) according to the previously described protocol (20). Gemcitabine (catalog No. S1714), 5FU (catalog No. S1209), niraparib (catalog No. S2741), A1155463 (catalog No. S7800), ABT199 (catalog No. S8048), S63845 (catalog No. S8383), and ABT263 (catalog No. S1001) were purchased from SelleckChem. All the compounds were dissolved in DMSO at 10 mmol/L stock solution for *in vitro* assays.

CRISPR screening using the therapeutic genome (RxG) library

Briefly, we designed a custom sgRNA library, the RxG library, targeting 996 genes for which therapeutic interventions have been identified (Supplementary Methods and Supplementary Excel File). We carried out CRISPR screens with the RxG library in the AsPC-1 cell line to identify candidate genes, which when targeted for disruption modulate sensitivity to three chemotherapeutics, gemcitabine, 5FU, and niraparib. Each screen was carried out in triplicate (IC_{30}-IC_{50} of each drug) for 16 days (T_{16D}) at approximately 500X library coverage. Triplicate puromycin selected samples (T_0 PURO) prior to exposure without treatment were collected as controls. Cells from each screen were harvested, genomic DNA prepared, sgRNAs amplified, and quantified by next-generation sequencing (NGS). MAGeCK, which utilizes a-RRA (Robust Ranking Algorithm) to rank candidate genes, was used to identify candidate genes for which the corresponding sgRNAs showed significantly altered distribution between treated and T_0 PURO control samples (31). Additional details are provided in the Supplementary Methods, and the CRISPR screening raw data are accessible at Dryad (https://doi.org/10.5061/dryad.m905qfv22).

Animal studies

NOD-*scid* IL2Rgamma^{null} (NSG) mice aged 5 to 6 weeks were purchased from The Jackson Laboratory (Stock No. 005557). The mice were allowed to acclimatize for 1 week. Animals were housed in the Association for Assessment and Accreditation of Laboratory Animal Care (AAALAC)-accredited animal facilities at the University of Florida under pathogen-free conditions. All animals received food and water *ad libitum*. G-68 PDX cells at 5×10^6 per mouse in 50% Matrigel (catalog No. 356237, Corning) in PBS were injected subcutaneously (s.c.) into the right flank region of the NSG mice (30). Pancreatic cancer PDX models (G192-p4, G176-p4, and LM12-p3) were established and characterized by Dr. Trevino at the University of Florida, and were propagated in NSG mice as reported previously (32). The tumors were harvested after they reached 1,500 mm^3, cut into 2-mm fragments, and were implanted subcutaneously after submerging in Matrigel in additional NSG mice (32). Tumor size was measured twice a week with digital calipers, and tumor volume was calculated using the formula (length$\times$width$^2\times$0.5) as described previously (20). The animals were randomized into different treatment groups when the tumors reached 100 to 200 mm^3. Animals were treated with vehicle, gemcitabine [20 mg/kg, once a week (every 7 days), i.p.], DT2216 [15 mg/kg, every 4 days, i.p.] and a combination of gemcitabine and DT2216. Gemcitabine was dissolved in normal saline, and DT2216 was formulated in 50% phosal 50 PG, 45% miglyol 810N and 5% polysorbate 80. They were administered in 100 μL of vehicle (saline for gemcitabine and 50% phosal 50 PG, 45% miglyol 810N, and 5% polysorbate 80 for DT2216) per mouse. DT2216 treatment was initiated 2 days before gemcitabine treatment and continued as described previously. Mice were euthanized when they became moribund, or their tumor sizes reached humane endpoint as per Institutional Animal Care and Use Committee (IACUC) policy. For euthanasia, animals were sacrificed by CO_2 suffocation followed by cervical dislocation. The tumors were subsequently harvested, fixed in buffered formalin, and processed for histopathology.

Study approval

Animal procedures were performed in accordance with the rules of IACUC at the University of Florida. The primary human pancreatic

cancer G-68 and G-46 cell lines and G192-p4, LM12-p3 and G176-p4 human pancreatic cancer PDXs were generated from deidentified tissues collected from patients. Informed written consent for the collection, and use of the tissues for research was obtained from all patients, and the use of these patient-derived cells and tissues for this study was approved by the University of Florida Institutional Review Board.

Statistical analysis

For analysis of the means of three or more groups, ANOVA tests were performed. In the event that ANOVA justified *post hoc* comparisons between group means, the comparisons were conducted using Tukey multiple-comparisons test. A two-sided unpaired Student *t* test was used for comparisons between the means of two groups. Apoptosis and spheroid assays statistical analyses were done by two-way ANOVA with Tukey *post hoc* test. A Kaplan–Meier test was used for the survival analysis, and the data were statistically analyzed using the log-rank (Mantel–Cox) test. $P < 0.05$ was considered to be statistically significant.

All other methods are described in Supplementary Information due to space limitation.

Results

CRISPR screening with the RxG library found that targeting of *BCL2L1* increases sensitivity of AsPC-1 cells to gemcitabine, 5FU, and niraparib

We constructed the RxG library, which targets 996 human target genes for which a pharmaceutical modulator had been identified (Supplementary Methods; Supplementary Tables S1 and S2). We carried out CRISPR screening in AsPC-1 pancreatic cancer cells using the RxG library to identify druggable genes that modulate sensitivity/resistance of AsPC-1 cells to gemcitabine, 5FU, and niraparib. (**Fig. 1A**). Briefly, AsPC-1 cells were transduced with the RxG library, puromycin selected (T_0 PURO), and exposed to DMSO (vehicle), gemcitabine (3.2 μmol/L), 5FU (2.5 μmol/L), and niraparib (10 μmol/L) for 8 days in triplicate. Genomic DNA was isolated from each sample, sgRNA amplified, and the abundance of each sgRNA determined by next-generation sequencing. We assessed the depletion/enrichment of each gene in the treated samples as compared with the T_0 PURO control using the MAGeCK algorithm (**Fig. 1A**; Supplementary Methods). Strikingly, targeted disruption of *BCL2L1*, which encodes BCL-X_L, resulted in a significant reduction of AsPC-1 cells in gemcitabine-, 5FU-, and niraparib-treated samples but not in the DMSO-treated cells (**Fig. 1B–D**). These findings suggest that BCL-X_L may enhance resistance to these agents in AsPC-1 cells. These results agree with previous findings, demonstrating that BCL-X_L plays a crucial role in the development of chemoresistance in pancreatic cancer cells (5).

Expression of the BCL-2 family proteins in and sensitivity of pancreatic cancer cells to BH3 mimetics

To gain more insight into the role of the BCL-2 family of proteins in the development of chemoresistance in pancreatic cancer cells, we analyzed the Cancer Cell Line Encyclopedia (CCLE) database and found that *BCL2L1* mRNA is predominantly overexpressed in pancreatic cancer cell lines compared with the cell lines that were derived from other malignancies (Supplementary Fig. S1A). Similarly, when we evaluated the expression of the BCL-2 family of proteins in four commonly used pancreatic cancer cell lines (i.e., AsPC-1, BxPC-3, Mia PaCa-2, and PANC-1) and two newly

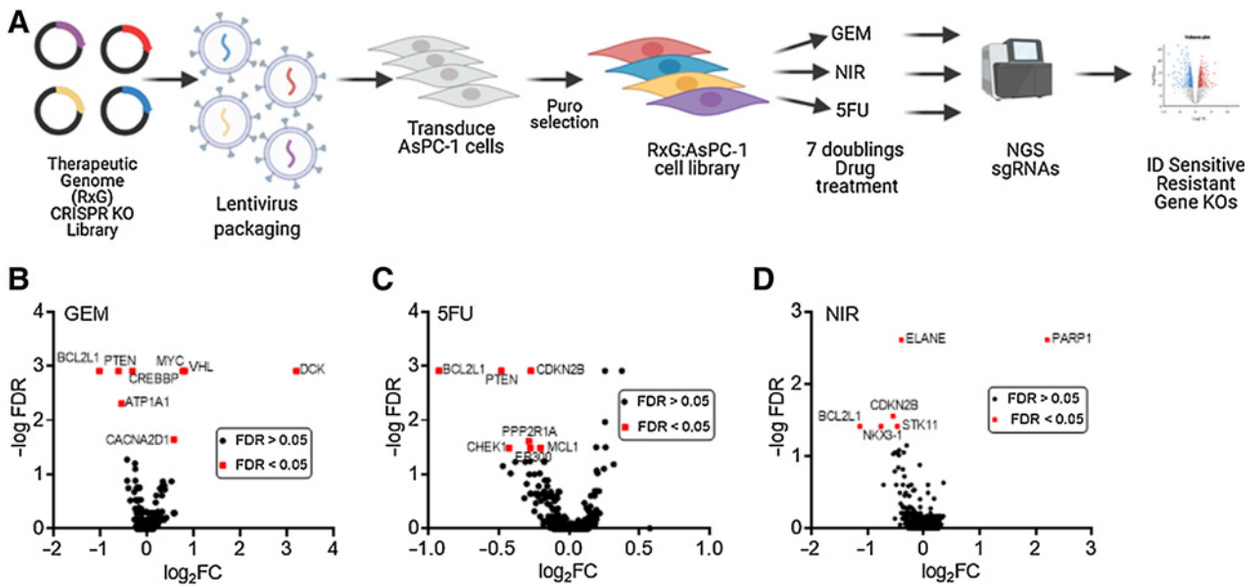

Figure 1.

BCL2L1 (BCL-X_L) provides resistance to gemcitabine treatment in pancreatic cancer. **A,** Representation of the Therapeutic Genome (RxG) CRISPR library screening to identify genes important for resistance to gemcitabine (GEM), 5FU, and niraparib (NIR) in the AsPC-1 pancreatic cancer cell line. **B–D,** Log_2 volcano plots showing the results of the screening for gemcitabine (**B**), 5FU (**C**), or niraparib (**D**). Several biologically interesting hits (including *BCL2L1*) identified from the screening are highlighted in red. Each gene targeted by the library was ranked based on the Model-based Analysis of Genome-wide CRISPR-Cas9 Knockout (MAGeCK) positive selection score. FDR, False discovery rate; FC, Fold change.

generated patient-derived primary pancreatic cancer cell lines (i.e., G-46 and G-68; Supplementary Table S3; ref. 30), we found that BCL-X_L and MCL-1 are abundantly expressed across all the pancreatic cancer cell lines, while BCL-2 expression was more variable (Supplementary Fig. S1B). Next, we determined the sensitivity of these pancreatic cancer cells to different BCL-2 family antiapoptotic protein inhibitors (commonly known as BH3 mimetics) including A1155463 (a BCL-X_L-selective inhibitor), ABT199 (a BCL-2-selective inhibitor), S63845 (an MCL-1-selective inhibitor), ABT263 (a dual BCL-X_L and BCL-2 inhibitor), and DT2216 (a BCL-X_L specific PROTAC or degrader) as single agents as well as in different combinations. All of the pancreatic cancer cell lines tested were found to be largely resistant to these inhibitors when used individually (Supplementary Fig. S1C), suggesting that unlike many leukemia and lymphoma cells, pancreatic cancer cells are not dependent on single BCL-2 family members for survival. Next, we tested different combinations of the BH3 mimetics and found that all of these pancreatic cancer cell lines were resistant to the combination of A1155463 and ABT199 as well as S63845 plus ABT199, but were highly sensitive to the combination of S63845 with any of these BCL-X_L–targeting agents including DT2216. However, MCL-1 inhibition causes severe toxicities including cardiotoxicity and hepatotoxicity, and these toxicities are exacerbated with dual targeting of MCL-1 and BCL-X_L (33–35). Hence, to avoid these toxicities, alternative pharmacologic agents that could cause MCL-1 suppression selectively in tumor cells would be of great importance to develop highly effective combination therapies with a platelet-sparing BCL-X_L–targeting agent such as DT2216 (23, 26).

A combination of gemcitabine and DT2216 synergistically kills pancreatic cancer cells *in vitro*

The priming of cancer cells to apoptosis with chemotherapeutic drugs has been shown to significantly increase the effectiveness of BCL-2 family inhibitors. In our RxG CRISPR screening, we identified that BCL-X_L plays a crucial role in the development of gemcitabine resistance. Thus, to improve the efficacy of gemcitabine, we investigated the potential to use the combination of gemcitabine and DT2216 for the treatment of pancreatic cancer.

First, we determined the effect of gemcitabine and DT2216 as single agents and in combination against different pancreatic cancer cell lines. Flow-cytometric analysis clearly showed that the combination of gemcitabine and DT2216 significantly increased apoptosis compared with the individual agents in four commonly used pancreatic cancer cell lines (AsPC-1, BxPC-3, Mia PaCa-2, and PANC-1; **Fig. 2A**, Supplementary Fig. S2A) as well as two newly generated patient-derived primary pancreatic cancer cell lines (G-68 and G-46; **Fig. 2B**; Supplementary Fig. S2B and S3A, B). We observed that, although, basal levels of BCL-X_L protein expression were different among the tested cell lines, all the cell lines were found to be sensitive to the combination of gemcitabine and DT2216, and that of gemcitabine and S63845 (**Fig. 2A** and **B**; Supplementary Fig. S1C), indicating that the efficacy of DT2216 may be independent of the basal expression of BCL-X_L. Furthermore, the combination of gemcitabine and DT2216 was found to synergistically reduce viability, colony formation, and tumor spheroid growth in the G-68 and G-46 cell lines (**Fig. 2C–G**; Supplementary Fig. S3C–S3G). These data confirm a synergistic interaction between gemcitabine and DT2216 against pancreatic cancer cells *in vitro*.

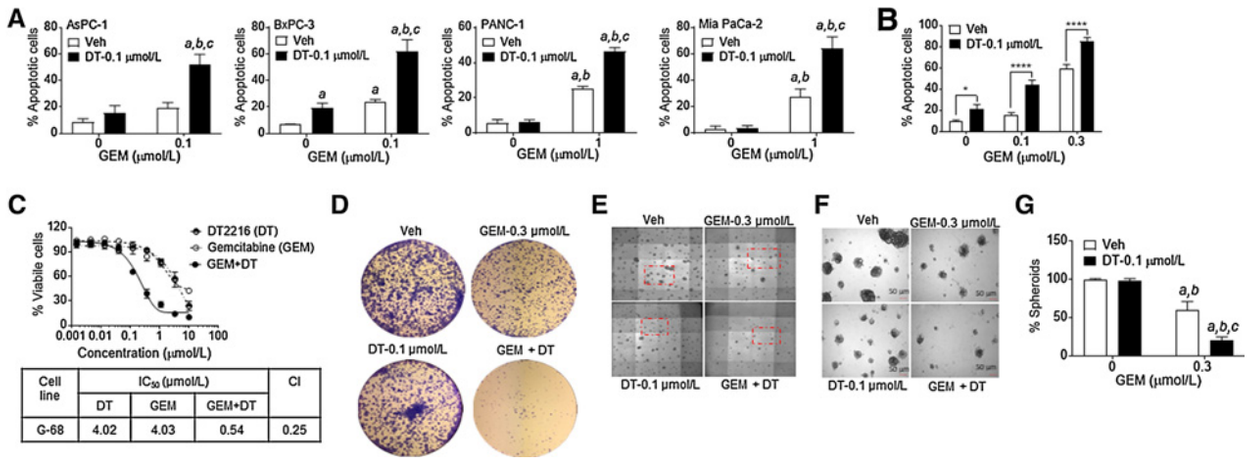

Cell line	IC_{50} (μmol/L)			CI
	DT	GEM	GEM+DT	
G-68	4.02	4.03	0.54	0.25

Figure 2.

The combination of DT2216 and gemcitabine synergistically kills pancreatic cancer cells *in vitro*. **A,** Percentage of total apoptotic cells (the sum of early [Annexin V^+] and late [PI^+/Annexin V^+] apoptotic cells) after the cells were treated with vehicle (Veh) or with the indicated concentrations of DT2216 (DT) or gemcitabine (GEM) alone or in combination for 72 hours. Data are presented as the mean ± SD of four independent experiments for each cell line and condition. **a**, **b** and **c,** $P < 0.05$ versus. Veh, DT and GEM, respectively. **B,** Percentage of total apoptotic G-68 primary pancreatic cancer cells after they were treated with vehicle (Veh) or the indicated concentrations of DT or gemcitabine alone or in combinations for 72 hours. Data are presented as mean ± SD ($n = 3$ independent experiments). *, $P < 0.05$; ****, $P <$ 0.0001. Representative flow cytometric quadruple graphs for **A** and **B** are shown in Supplementary Fig. S2A and S2B, respectively. **C,** Percentage viability of G-68 cells after they were treated with increasing concentrations of DT, gemcitabine, or their combination (GEM+DT; 1:1 ratio) for 72 hours. The table shows the IC_{50} values of DT, gemcitabine, or their combination (GEM+DT). IC_{50} values are shown for a representative experiment out of three independent experiments. The CI value (< 1) indicates a synergy between DT and gemcitabine. **D,** G-68 cells were treated with the indicated concentrations of DT or gemcitabine alone or in combination for 72 hours followed by incubation in drug-free medium for another two weeks. Crystal violet staining was performed to visualize the colonies. Data are representative images from two independent experiments. **E,** G-68 cells were seeded in a 48-well plate and allowed 48 hours for spheroid formation before DT and/or gemcitabine treatment. Micrographs (magnification at 50×) of spheroids in the corresponding wells after they were treated with the indicated concentrations of DT or gemcitabine alone or in combination for 10 days are shown**. F,** Microphotographs (magnification 50×) of spheroids from the marked areas in **E**. **G,** Quantification of the number of spheroids from **E** as a percentage of Veh. **a**, **b** and **c,** $P < 0.05$ versus Veh, DT, and GEM, respectively. Data presented in **E–G** are representative of three independent experiments. Statistical significance in **A**, **B**, and **G** was determined by two-way ANOVA with Tukey *post hoc* test.

BCL-X_L degradation by DT2216 increases MCL-1 dependence and sensitivity to gemcitabine in pancreatic cancer cells

Having established the synergistic activity of gemcitabine and DT2216 against pancreatic cancer cells *in vitro*, we next sought to uncover the molecular mechanisms behind their synergy. We chose the G-68 cell line for these mechanistic studies because it is a primary pancreatic cancer cell line from a patient with a T3N1 tumor harboring both the KRASG12D and TP53R248W mutations. It resembles invasive pancreatic cancer in patients more than the commonly used human pancreatic cancer cell lines (30). DT2216 potently degraded BCL-X_L in a concentration-dependent manner without any significant effect on BCL-2 and MCL-1 (**Fig. 3A**). On the other hand, gemcitabine treatment significantly downregulated MCL-1 protein expression and partially downregulated BCL-X_L in a concentration-dependent manner, while BCL-2 levels were not affected. In addition, gemcitabine also increased the expression of NOXA that selectively binds MCL-1 to induce apoptosis (**Fig. 3B**; ref. 36). Next, we analyzed the effect of the gemcitabine-DT2216 combination on BCL-2 family members and apoptosis markers. We found that the combination reduced the levels of MCL-1 and BCL-X_L in the cells. Furthermore, apoptosis markers such as cleaved-caspase 3 and cleaved-PARP levels were significantly increased with the combination treatment compared with treatment with the individual agents (**Fig. 3C**). This enhanced effectiveness of the combination treatment further supports the codependency of these cells on BCL-X_L and MCL-1. Next, we determined whether differential binding of BIM to BCL-X_L and MCL-1 was the reason for the limited single-agent activity in pancreatic cancer cells. To directly compare the binding of BIM to BCL-X_L and MCL-1, we performed immunoprecipitation of BCL-X_L and MCL-1. We observed that at the baseline, BIM is more associated with BCL-X_L, whereas degradation of BCL-X_L by DT2216 led to its increased association with MCL-1 (**Fig. 3D**, **E**). This confirms that BCL-X_L degradation by DT2216 increases MCL-1 dependence and could be a reason for the limited activity of a single agent. Together, downregulation of MCL-1 by gemcitabine under DT2216 treatment confirmed the mechanism behind the combination effect. The codependency of pancreatic cancer cells on BCL-X_L and MCL-1 was further validated using cell viability assays utilizing an MCL-1-specific inhibitor (S63845) and DT2216 (**Fig. 3F** and Supplementary Fig. S1C). Collectively, our data suggest that gemcitabine-induced MCL-1 downregulation with BCL-X_L degradation by DT2216 may be primarily responsible for this synthetic lethality in pancreatic cancer cells. Furthermore, RT-PCR analysis showed that the altered protein expression of BCL-2 family members in the combination treatment is not associated with changes in mRNA levels (**Fig. 3G** and Supplementary Table S4).

Combination of gemcitabine and DT2216 can more effectively suppress the growth of G-68 xenografts and PDX tumors than either agent alone in mice

Given the excellent synergetic activity in pancreatic cancer cells *in vitro*, we sought to evaluate the effect of gemcitabine and DT2216 *in vivo*. Xenograft tumor models were established using the G-68 cell line. Tumor-bearing NOD-*scid* IL2Rg^{null} (NSG) mice were randomized into four groups ($n = 7$ mice per group) once the tumors reached

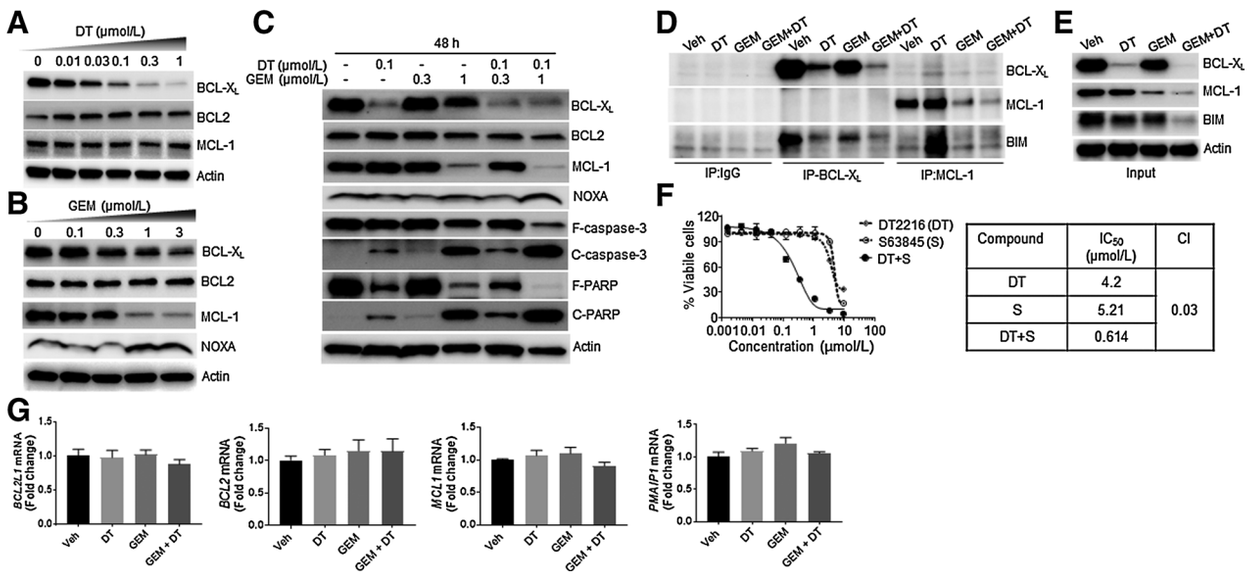

Figure 3.

Synergy between DT2216 and gemcitabine attributes to a combined depletion of BCL-X_L and MCL-1. **A,** Immunoblot analysis of BCL-X_L, BCL-2, and MCL-1 in G-68 cells after they were treated with the indicated concentrations of DT2216 (DT) for 16 hours. **B,** Immunoblot analysis of BCL-X_L, BCL-2, MCL-1, and NOXA in G-68 cells after they were treated with the indicated concentrations of gemcitabine (GEM) for 48 hours. **C,** Immunoblot analysis of BCL-X_L, BCL-2, MCL-1, NOXA, and apoptosis markers – cleaved (**C**) and full-length caspase-3 and PARP in G-68 cells after they were treated with the indicated concentrations of gemcitabine and/or DT for 48 hours. Immunoblots presented in **A-C** are representative of three independent experiments. **D,** G-68 cells were treated with gemcitabine (1 μmol/L) and/or DT (0.1 μmol/L) for 48 hours. Cell lysates were subjected to co-immunoprecipitation (Co-IP) using BCL-X_L or MCL-1 antibodies followed by immunoblotting to detect BCL-X_L, MCL-1, and BIM. **E,** The levels of BCL-X_L, MCL-1, and BIM in the inputs for **D**. β-actin was used as an equal loading control for all immunoblot analyses presented in **A–E**. **F,** Viability of G-68 cells after they were treated with increasing concentrations of DT or S63845 (S) individually or in combination (DT+S) for 72 hours. IC_{50} values are shown in the table. The CI value indicates a synergy between DT and S. **G,** G-68 cells were treated with 0.1 μmol/L of DT or 1 μmol/L of gemcitabine alone or in combination (gemcitabine + DT) for 48 hours. The fold changes in the expressions of *BCL2L1* (encodes BCL-X_L), *BCL2*, *MCL1*, and *PMAIP1* (encodes NOXA) mRNA are shown. *GAPDH* was used as an internal control. Data are from a single experiment performed in triplicate (mean ± SD).

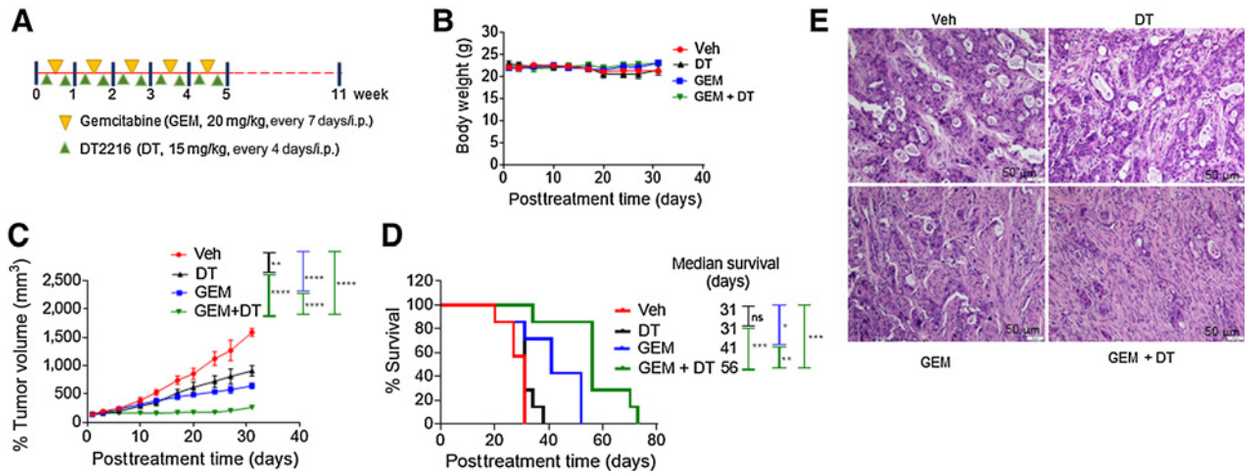

Figure 4.

DT2216 increased the antitumor efficacy of gemcitabine in a patient-derived G-68 pancreatic cancer cell xenograft model. **A,** Representation of the experimental design of the G-68 xenograft study. Tumor-bearing mice were administered Veh, DT2216 (DT), gemcitabine (GEM), or a combination of DT and gemcitabine at the indicated dosing regimen. **B,** Change in body weight during the course of treatment. **C,** Graph showing the tumor volume changes in each group after the start of treatment until the control animals were euthanized. Data are presented as mean ± SEM ($n = 7$ mice in each group at the start of treatment). Statistical significance was determined by unpaired two-sided Student *t* test test. **, $P < 0.01$; ****, $P < 0.0001$. **D,** Kaplan–Meier survival analysis with medium survival time of mice in each group. Statistical significance was determined by Mantel–Cox test. *, $P < 0.05$; **, $P < 0.01$; ***, $P < 0.001$. **E,** Representative H&E staining images of tumors in each treatment group at 200x magnification, scale bar = 50 μm.

100 to 200 mm^3. The animals were treated intraperitoneally (i.p.) with vehicle, gemcitabine (20 mg/kg, every 7 days), DT2216 (15 mg/kg, every 4 days), or the combination of gemcitabine and DT2216 (**Fig. 4A**). In this model, gemcitabine was slightly more effective than DT2216 in inhibiting tumor growth and increasing the survival of the tumor-bearing mice, whereas the combination treatment was more effective than either agent alone without any significant decrease in body weight (**Fig. 4B–E**). Previous reports have shown that a combination of BCL-X_L and MCL-1 inhibitors induced acute hepatotoxicity in mice (34). Thus, we studied the histopathology of the liver, heart, and kidney in mice receiving the individual treatments or the combination therapy and found no evidence of any organ toxicity, which is in agreement with the observation that there was no body weight change during the treatments (Supplementary Fig. S4A).

Recently, it has been shown that PDX tumor models can better recapitulate tumor biology, stromal content, genetic mutations, and heterogeneity of human diseases than conventional tumor xenograft models employing cancer cell lines (37). They are also more predictive of clinical outcomes of experimental therapeutic agents than the latter (37). We have established a number of pancreatic cancer PDX models and selected G192-p4, G176-p4, and LM12-p3 human pancreatic cancer PDX models to further evaluate the therapeutic efficacy of gemcitabine and DT2216 alone or in combination (**Fig. 5A**; Supplementary Table S5; refs. 32, 38, 39). In the G192-p4 PDX model, the combination treatment significantly inhibited tumor growth compared with monotherapy of gemcitabine or DT2216 (**Fig. 5B**). In addition, histopathology from the G192-p4 PDX model showed a significant decrease in tumor burden in mice treated with the combination, and no evidence of organ toxicity was observed in the liver, kidney, or heart (**Fig. 5C** and Supplementary Fig. S4B). The combination of gemcitabine and DT2216 was also more effective in inhibiting tumor growth in the G176-p4 model than either agent alone (**Fig. 5D**). In LM12-p3 PDX, the combination treatment caused more reduction in tumor volume than either treatment alone, but the difference was not statistically significant (**Fig. 5E**). Interestingly, DT2216 was equally effective in degrading BCL-X_L in tumors harvested from all these PDXs (Supplementary Fig. S5A), which suggests that the differential efficacy of the combination against these PDXs may not be attributed to differential BCL-X_L degradation. In fact, the efficacy of the combination appears to be correlated with MCL-1 expression in these PDXs, that is, PDXs with high MCL-1 expression (G192-p4) responded best to the treatment (Supplementary Fig. S5B). In addition, the heterogeneity of the PDXs may also contribute to the differences of their responses to the combination therapy. In fact, LM12-p3 PDX tumor tissues were derived from an aggressive liver metastasis, and thus appeared more resistant to any of these treatments than the other two PDXs (**Fig. 5**). Together, these data illustrate that the combination of gemcitabine and DT2216 is potentially a more effective treatment for some pancreatic cancers than gemcitabine alone. Future studies will be needed to identify biomarkers that can be used to stratify pancreatic cancer patients for this combination therapy.

Discussion

Pancreatic cancer is a difficult-to-treat cancer with gemcitabine as a current first-line standard of care. Unfortunately, gemcitabine is ineffective to treat this deadly disease because of development of drug resistance (4–7). The current studies emanate from the fact that BCL-X_L is the most highly expressed gene in pancreatic cancer as analyzed through the CCLE transcriptomics database. We found that compared to BCL-2, the expression of BCL-X_L is high in all the pancreatic cancer cells examined in our study. The importance of BCL-X_L in the progression of PanIN to PDAC has also been demonstrated by others in pancreas-specific $Kras^{G12D}$ (P-$Kras^{G12D}$) mice (12). A recent study showed that ABT263 increased the antitumor effect of prexasertib, a Chk1 inhibitor, by inducing apoptosis in pancreatic cancer cells via inhibition of BCL-X_L but not BCL-2 (40). Furthermore, Zhang Z and colleagues showed that GATA1 induced gemcitabine resistance in pancreatic cancer cells through the upregulation of BCL-X_L

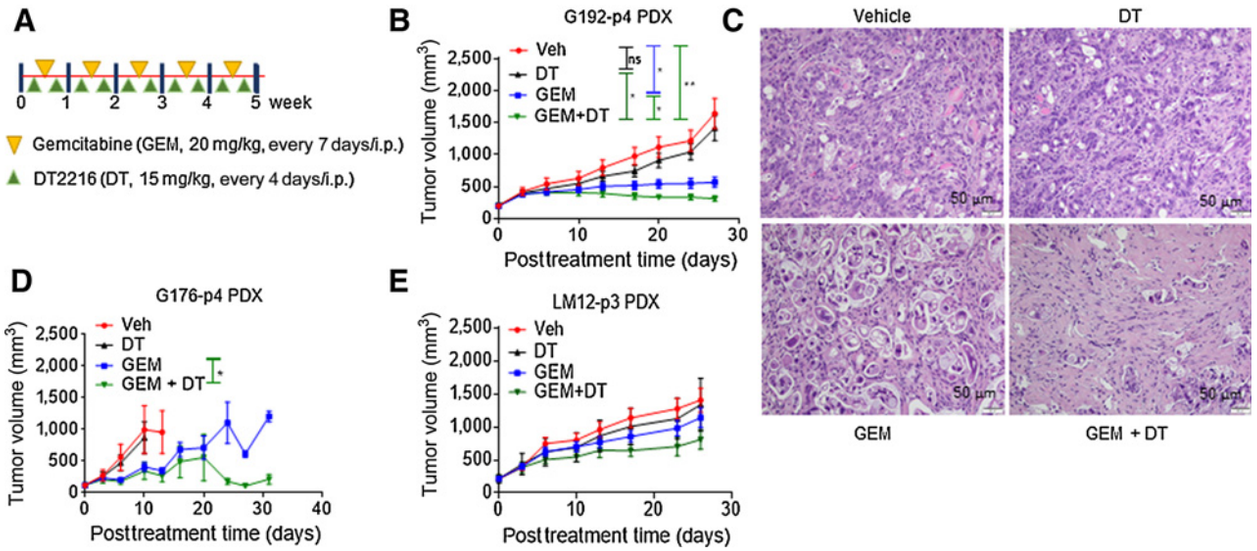

Figure 5.

DT2216 increased the antitumor efficacy of gemcitabine in pancreatic cancer PDX models. **A,** Representation of the experimental design of the PDX studies. Tumor-bearing mice were administered Veh, DT2216 (DT), gemcitabine (GEM), or a combination of DT and gemcitabine at the indicated dosing regimen. **B,** Graph showing the tumor volume changes in G192-p4 PDXs in each group after the start of treatment. **C,** Representative H&E staining images of G192-p4 PDX tumors in each treatment group at 200 × magnification, scale bar = 50 μm. **D** and **E,** Graphs showing the tumor volume changes in G176-p4 (**D**) and LM12-p3 (**E**) PDXs in each group after the start of treatment. The data presented in (**B**), (**D**) and **E** are mean ± SEM (n = 7 mice in each group at the start of treatment). Statistical significance was determined by unpaired two-sided Student t test. *, $P < 0.05$; **, $P < 0.01$; ns, not significant.

expression (41). Using the RxG CRISPR screening, we identified BCL-X_L as the most common gene providing resistance to not only gemcitabine, but also to other chemotherapeutics such as 5FU and NIR. These findings confirm that BCL-X_L is involved in the development of therapeutic resistance in pancreatic cancer and is a potential key druggable pancreatic cancer target.

Since on-target thrombocytopenia is a major hurdle in the clinical development of BCL-X_L inhibitors, we recently adopted a novel PROTAC technology to overcome this toxicity by converting ABT263 (BCL-X_L/2 dual inhibitor) into a BCL-X_L selective PROTAC, named DT2216 (20–22). DT2216 is currently in phase I clinical studies for patients with relapsed/refractory malignancies (NCT04886622). In the current study, through a series of *in vitro* assays and *in vivo* studies including the use of our newly established patient-derived primary pancreatic cancer cells lines and PDX models, we confirmed that DT2216 can sensitize pancreatic cancer cells to gemcitabine. These results suggest that the gemcitabine–DT2216 combination is a promising new therapy against pancreatic cancer, which will be useful to guide the clinical development of DT2216.

The mechanism by which gemcitabine and DT2216 can synergistically kill pancreatic cancer cells is because they can simultaneously target MCL-1 and BCL-X_L. Pancreatic cancer cells express high levels of not only BCL-X_L but also MCL-1 and are thus insensitive to individual inhibition of BCL-X_L or MCL-1. Therefore, like many other solid tumor cells, pancreatic cancer cells respond poorly to BCL-2 family inhibitors when used as a single agent treatment (23–26). Cotargeting BCL-X_L and MCL-1 with their respective inhibitors shows synergistic killing of most of the pancreatic cancer cell lines. Similarly, a combination of ABT263 and S63845 has shown increased antitumor activity in melanoma and lung cancers (34, 42). Unfortunately, the toxicities (including cardiotoxicity and hepatotoxicity) associated with dual inhibition of BCL-X_L and MCL-1 are a major challenge for clinical development of this combination (33–35). Therefore, an agent that could selectively target MCL-1 in tumor cells combined with a platelet-sparing BCL-X_L targeting agent such as DT2216 has the potential to overcome the toxicities and provide a more effective treatment of pancreatic cancer. Our results show that the degradation of BCL-X_L by DT2216 increased the dependency of pancreatic cancer cells on MCL-1 due to interaction with BIM. This likely explains the limited single-agent activity of DT2216 in pancreatic cancer. Interestingly, gemcitabine inhibited the expression of MCL-1 in pancreatic cancer cells. Therefore, MCL-1 downregulation by gemcitabine and BCL-X_L degradation by DT2216 may contribute to the synergistic effect of their combination against pancreatic cancer cells *in vitro* and *in vivo*. However, unlike the combination treatment with of BCL-X_L and MCL-1 inhibitors, which caused acute liver toxicity in mice (34), the combination of gemcitabine and DT2216 did not change the body weight of tumor-bearing mice, nor did it cause any observable tissue damage in the liver, kidney, and heart from these mice. This finding suggests that gemcitabine may selectively downregulate MCL-1 expression in pancreatic cancer cells, which could avoid the induction of systemic toxicities when combined with DT2216.

One of the advantages of using PDX tumor models to test new therapeutic agents and strategies is that PDX tumor models can recapitulate the heterogeneity of human diseases better than conventional tumor xenograft models employing long-term established cancer cell lines, and thus the findings in PDX tumor models are more predictive of clinical outcomes of experimental therapeutic agents than the latter (37). Indeed, we found that even though the pancreatic cancer xenograft model generated with the patient-derived primary G-68 pancreatic cancer cells showed moderate sensitivity to DT2216, DT2216 alone did not induce any significant response in any of the three PDX models tested in our study. Moreover, the responses of these PDX models to gemcitabine alone and the combination of gemcitabine and DT2216 were also highly variable. For example, gemcitabine alone

almost completely inhibited the tumor growth in mice bearing G192-p4 PDX, and the combination of gemcitabine and DT2216 induced significant tumor regression. In contrast, although the combination of gemcitabine and DT2216 caused a greater inhibition of LM12-p3 PDX growth compared to single agents, the difference was not statistically significant. The mechanisms underlying these different responses to the treatments have yet to be determined but are unlikely attributable to their differential expression of the BCL-2 anti-apoptotic family proteins as shown in other malignancies (43). It will be of a great interest to determine whether BH3 profiling can be used to predict the responses of different pancreatic cancer PDXs and patients with pancreatic cancer to the treatment with gemcitabine and DT2216 (44). This information could be useful in stratifying the patients that could benefit from this combination.

In conclusion, we identified BCL-X_L as a key anti-apoptotic protein in pancreatic cancer that limits the therapeutic efficacy of gemcitabine. Furthermore, we demonstrated that DT2216 significantly improved the effectiveness of gemcitabine against pancreatic cancer cells *in vitro* and in PDX models without causing observable normal tissue toxicity. These findings suggest that the combination of DT2216 and gemcitabine has the potential to be developed as a safe and effective combination therapy for pancreatic cancer.

Authors' Disclosures

D. Thummuri reports grants from the NIH during the conduct of the study and has a patent for Therapeutic Agents and Methods of Treatment pending and with royalties paid. S. Khan reports grants from University of Florida during the conduct of the study; and has a patent for BCL-2 Proteins Degraders for Cancer Treatment pending and with royalties paid. P. Zhang reports a patent for WO2020163823A2 issued, licensed, and with royalties paid from Dialectic Therapeutics and a patent for WO2019144117A1 issued, licensed, and with royalties paid from Dialectic Therapeutics. J. Wiegand reports grants from the NIH during the conduct of the study. X. Zhang reports a patent 1 pending and a patent 2 pending. A. Tagmount reports other support from University of Florida, College of Medicine Pilot Funds during the conduct of the study. A.N. Riner reports grants from the NIH during the conduct of the study. R. Hromas reports he has equity in Dialectic Therapeutics, which has licensed the compounds described herein. C.D. Vulpe reports other support from University of Florida, College of Medicine Pilot Funds during the conduct of the study. G. Zheng reports grants and other support from Dialectic Therapeutics outside the submitted work, has a patent for WO 2017184995 issued to Dialectic Therapeutics, and a patent for WO 2019144117 issued to Dialectic Therapeutics. D. Zhou reports other support from Dialectic Therapeutics during the conduct of the study; other support from Dialectic Therapeutics outside the submitted work; and has a patent for PCT/US17/28875 issued, licensed, and with royalties paid from Dialectic Therapeutics. No disclosures were reported by the other authors.

Authors' Contributions

D. Thummuri: Conceptualization, data curation, formal analysis, validation, investigation, visualization, methodology, writing–original draft, writing–review and editing. **S. Khan:** Conceptualization, data curation, formal analysis, validation, investigation, visualization, methodology, writing–original draft, writing–review and editing. **P.W. Underwood:** Conceptualization, resources, methodology, writing–review and editing. **P. Zhang:** Resources. **J. Wiegand:** Data curation, investigation, methodology, writing–review and editing. **X. Zhang:** Resources. **V. Budamagunta:** Data curation. **A. Sobh:** Data curation, formal analysis. **A. Tagmount:** Data curation, formal analysis. **A. Loguinov:** Data curation, formal analysis. **A.N. Riner:** Resources, data curation, formal analysis, writing–review and editing. **A.S. Akki:** Data curation, formal analysis, visualization, writing–review and editing. **E. Williamson:** Data curation, formal analysis. **R. Hromas:** Conceptualization, formal analysis, supervision, funding acquisition, writing–review and editing. **C.D. Vulpe:** Conceptualization, formal analysis, supervision, funding acquisition, investigation, visualization, methodology, writing–original draft. **G. Zheng:** Resources, formal analysis, supervision, funding acquisition, writing–review and editing. **J.G. Trevino:** Conceptualization, resources, formal analysis, supervision, funding acquisition, investigation, methodology, writing–review and editing. **D. Zhou:** Conceptualization, formal analysis, supervision, funding acquisition, writing–original draft, writing–review and editing.

Acknowledgments

The authors thank Alexandra M. Fahnlander for her editorial assistance. This study was supported in part by US National Institutes of Health (NIH) grants R01 CA242003 (to D. Zhou, J.G. Taverno, and G. Zheng), RO1 CA CA205224 (to R. Hromas) and T32 HG008958 (to A.N. Riner).

The costs of publication of this article were defrayed in part by the payment of page charges. This article must therefore be hereby marked *advertisement* in accordance with 18 U.S.C. Section 1734 solely to indicate this fact.

Received May 28, 2021; revised August 16, 2021; accepted October 14, 2021; published first October 19, 2021.

References

1. Bray F, Ferlay J, Soerjomataram I, Siegel RL, Torre LA, Jemal A. Global cancer statistics 2018: GLOBOCAN estimates of incidence and mortality worldwide for 36 cancers in 185 countries. CA Cancer J Clin 2018;68:394–424.
2. Grossberg AJ, Chu LC, Deig CR, Fishman EK, Hwang WL, Maitra A, et al. Multidisciplinary standards of care and recent progress in pancreatic ductal adenocarcinoma. CA Cancer J Clin 2020;70:375–403.
3. Tempero MA, Malafa MP, Al-Hawary M, Asbun H, Bain A, Behrman SW, et al. Pancreatic adenocarcinoma, version 2.2017, NCCN clinical practice guidelines in oncology. J Natl Compr Canc Netw 2017;15:1028–61.
4. Quinonero F, Mesas C, Doello K, Cabeza L, Perazzoli G, Jimenez-Luna C, et al. The challenge of drug resistance in pancreatic ductal adenocarcinoma: a current overview. Cancer Biol Med 2019;16:688–99.
5. Schniewind B, Christgen M, Kurdow R, Haye S, Kremer B, Kalthoff H, et al. Resistance of pancreatic cancer to gemcitabine treatment is dependent on mitochondria-mediated apoptosis. Int J Cancer 2004;109:182–8.
6. Choi S, Chen Z, Tang LH, Fang Y, Shin SJ, Panarelli NC, et al. Bcl-xL promotes metastasis independent of its anti-apoptotic activity. Nat Commun 2016;7:10384.
7. Yang G, Guan W, Cao Z, Guo W, Xiong G, Zhao F, et al. Integrative genomic analysis of gemcitabine resistance in pancreatic cancer by patient-derived xenograft models. Clin Cancer Res 2021;;27:3383–96.
8. Neoptolemos JP, Kleeff J, Michl P, Costello E, Greenhalf W, DH P, et al. Therapeutic developments in pancreatic cancer: current and future perspectives. Nat Rev Gastroenterol Hepatol 2018;15:333–48.
9. Conroy T, Hammel P, Hebbar M, Ben Abdelghani M, Wei AC, Raoul J-L, et al. FOLFIRINOX or gemcitabine as adjuvant therapy for pancreatic cancer. N Engl J Med 2018;379:2395–406.
10. Bauer C, Hees C, Sterzik A, Bauernfeind F, Mak'Anyengo R, Duewell P, et al. Proapoptotic and antiapoptotic proteins of the Bcl-2 family regulate sensitivity of pancreatic cancer cells toward gemcitabine and T-cell-mediated cytotoxicity. J Immunother 2015;38:116–26.
11. Corcoran RB, Cheng KA, Hata AN, Faber AC, Ebi H, Coffee EM, et al. Synthetic lethal interaction of combined BCL-XL and MEK inhibition promotes tumor regressions in KRAS mutant cancer models. Cancer Cell 2013;23:121–8.
12. Ikezawa K, Hikita H, Shigekawa M, Iwahashi K, Eguchi H, Sakamori R, et al. Increased Bcl-xL expression in pancreatic neoplasia promotes carcinogenesis by inhibiting senescence and apoptosis. Cell Mol Gastroenterol Hepatol 2017;4:185–200.e1.
13. Miyamoto Y, Hosotani R, Wada M, Lee J-U, Koshiba T, Fujimoto K, et al. Immunohistochemical analysis of Bcl-2, Bax, Bcl-X, and Mcl-1 expression in pancreatic cancers. Oncology 1999;56:73–82.
14. Masui T, Hosotani R, Ito D, Kami K, Koizumi M, Mori T, et al. Bcl-XL antisense oligonucleotides coupled with antennapedia enhances radiation-induced apoptosis in pancreatic cancer. Surgery 2006;140:149–60.
15. Kasai S, Sasaki T, Watanabe A, Nishiya M, Yasuhira S, Shibazaki M, et al. Bcl-2/Bcl-xL inhibitor ABT-737 sensitizes pancreatic ductal adenocarcinoma to paclitaxel-induced cell death. Oncol Lett 2017;14:903–8.

16. Bai J, Sui J, Demirjian A, Vollmer CM, Jr., Marasco W, Callery MP. Predominant Bcl-XL knockdown disables antiapoptotic mechanisms: tumor necrosis factor-related apoptosis-inducing ligand-based triple chemotherapy overcomes chemoresistance in pancreatic cancer cells in vitro. Cancer Res 2005;65:2344–52.
17. Masood A, Azmi AS, Mohammad RM. Small molecule inhibitors of bcl-2 family proteins for pancreatic cancer therapy. Cancers (Basel) 2011;3:1527–49.
18. Kaefer A, Yang J, Noertersheuser P, Mensing S, Humerickhouse R, Awni W, et al. Mechanism-based pharmacokinetic/pharmacodynamic meta-analysis of navitoclax (ABT-263) induced thrombocytopenia. Cancer Chemother Pharmacol 2014;74:593–602.
19. Gandhi L, Camidge DR, Ribeiro De Oliveira M, Bonomi P, Gandara D, Khaira D, et al. Phase i study of navitoclax (ABT-263), a novel bcl-2 family inhibitor, in patients with small-cell lung cancer and other solid tumors. J Clin Oncol 2011;29: 909–16.
20. Khan S, Zhang X, Lv D, Zhang Q, He Y, Zhang P, et al. A selective BCL-XL PROTAC degrader achieves safe and potent antitumor activity. Nat Med 2019; 25:1938–47.
21. He Y, Koch R, Budamagunta V, Zhang P, Zhang X, Khan S, et al. DT2216—a Bcl-xL-specific degrader is highly active against Bcl-xL-dependent T cell lymphomas. J Hematol Oncol 2020;13:95.
22. Kolb R, De U, Khan S, Luo Y, Kim M-C, Yu H, et al. Proteolysis-targeting chimera against BCL-XL destroys tumor-infiltrating regulatory T cells. Nat Commun 2021;12:1281.
23. Corcoran RB, Cheng KA, Hata AN, Faber AC, Ebi H, Coffee EM, et al. Synthetic lethal interaction of combined BCL-XL and MEK inhibition promotes tumor regressions in KRAS mutant cancer models. Cancer Cell 2013;23:121–8.
24. Faber AC, Coffee EM, Costa C, Dastur A, Ebi H, Hata AN, et al. mTOR inhibition specifically sensitizes colorectal cancers with KRAS or BRAF mutations to BCL-2/BCL-XL inhibition by suppressing MCL-1. Cancer Discov 2014;4:42–52.
25. Nangia V, Siddiqui FM, Caenepeel S, Timonina D, Bilton SJ, Phan N, et al. Exploiting MCL1 dependency with combination MEK + MCL1 inhibitors leads to induction of apoptosis and tumor regression in KRAS-mutant non–small cell lung cancer. Cancer Discov 2018;8:1598–613.
26. Faber AC, Farago AF, Costa C, Dastur A, Gomez-Caraballo M, Robbins R, et al. Assessment of ABT-263 activity across a cancer cell line collection leads to a potent combination therapy for small-cell lung cancer. Proc Natl Acad Sci 2015; 112:E1288-E1296.
27. Morales AA, Kurtoglu M, Matulis SM, Liu J, Siefker D, Gutman DM, et al. Distribution of Bim determines Mcl-1 dependence or codependence with Bcl-xL/Bcl-2 in Mcl-1–expressing myeloma cells. Blood 2011;118:1329–39.
28. Korfi K, Smith M, Swan J, Somervaille TCP, Dhomen N, Marais R., BIM mediates synergistic killing of B-cell acute lymphoblastic leukemia cells by BCL-2 and MEK inhibitors. Cell Death Dis 2016;7:e2177–.
29. Pham K, Delitto D, Knowlton AE, Hartlage ER, Madhavan R, Gonzalo DH, et al. Isolation of pancreatic cancer cells from a patient-derived xenograft model allows for practical expansion and preserved heterogeneity in culture. Am J Pathol 2016;186:1537–46.
30. Principe DR, Narbutis M, Kumar S, Park A, Viswakarma N, Dorman MJ, et al. Long-term gemcitabine treatment reshapes the pancreatic tumor microenvironment and sensitizes murine carcinoma to combination immunotherapy. Cancer Res 2020;80:3101–15.
31. Li W, Xu H, Xiao T, Cong L, Love MI, Zhang F, et al. MAGeCK enables robust identification of essential genes from genome-scale CRISPR/Cas9 knockout screens. Genome Biol 2014;15:554.
32. Kazi A, Chen LW, Xiang SY, Vangipurapu R, Yang H, Beato F, et al. Global phosphoproteomics reveal CDK suppression as a vulnerability to KRas addiction in pancreatic cancer. Clin Cancer Res 2021;27:4012–24.
33. Hikita H, Takehara T, Shimizu S, Kodama T, Li W, Miyagi T, et al. Mcl-1 and Bcl-xL cooperatively maintain integrity of hepatocytes in developing and adult murine liver. Hepatology 2009;50:1217–26.
34. Weeden CE, Ah-Cann C, Holik AZ, Pasquet J, Garnier J-M, Merino D, et al. Dual inhibition of BCL-XL and MCL-1 is required to induce tumour regression in lung squamous cell carcinomas sensitive to FGFR inhibition. Oncogene 2018;37: 4475–88.
35. Thomas RL, Roberts DJ, Kubli DA, Lee Y, Quinsay MN, Owens JB, et al. Loss of MCL-1 leads to impaired autophagy and rapid development of heart failure. Genes Dev 2013;27:1365–77.
36. Ploner C, Kofler R, Villunger A. Noxa: at the tip of the balance between life and death. Oncogene 2008;27:S84–92.
37. Hidalgo M, Amant F, Biankin AV, Budinská E, Byrne AT, Caldas C, et al. Patient-derived xenograft models: an emerging platform for translational cancer research. Cancer Discov 2014;4:998–1013.
38. Inkoom A, Ndemazie N, Affram K, Smith T, Zhu X, Underwood P, et al. Enhancing efficacy of gemcitabine in pancreatic patient-derived xenograft mouse models. Int J Pharm X 2020;2:100056.
39. Go KL, Delitto D, Judge SM, Gerber MH, George TJ, Behrns KE, et al. Orthotopic patient-derived pancreatic cancer xenografts engraft into the pancreatic parenchyma, metastasize, and induce muscle wasting to recapitulate the human disease. Pancreas 2017;46:813–9.
40. Morimoto Y, Takada K, Takeuchi O, Watanabe K, Hirohara M, Hamamoto T, et al. Bcl-2/Bcl-xL inhibitor navitoclax increases the antitumor effect of Chk1 inhibitor prexasertib by inducing apoptosis in pancreatic cancer cells via inhibition of Bcl-xL but not Bcl-2. Mol Cell Biochem 2020;472:187–98.
41. Chang Z, Zhang Y, Liu J, Guan C, Gu X, Yang Z, et al. GATA1 promotes gemcitabine resistance in pancreatic cancer through antiapoptotic pathway. J Oncol 2019;2019:9474273.
42. Lee EF, Harris TJ, Tran S, Evangelista M, Arulananda S, John T, et al. BCL-XL and MCL-1 are the key BCL-2 family proteins in melanoma cell survival. Cell Death Dis 2019;10:342.
43. Koch R, Christie AL, Crombie JL, Palmer AC, Plana D, Shigemori K, et al. Biomarker-driven strategy for MCL1 inhibition in T-cell lymphomas. Blood 2019;133:566–75.
44. Montero J, Sarosiek KA, DeAngelo JD, Maertens O, Ryan J, Ercan D, et al. Drug-induced death signaling strategy rapidly predicts cancer response to chemotherapy. Cell 2015;160:977–89.